Comparison of standardized uptake values in normal structures and breast cancer metastases using PET/CT and PET/MRI

Akshat C Pujara[1], Carolyn Wassong[1], Roy A Raad[1], James Babb[1], Linda Moy[1], and Amy Melsaether[1]
[1]*New York University School of Medicine, New York, NY, United States*

Target Audience: Radiologists and basic scientists interested in methods and multi-organ system performance of 18-FDG PET/MRI for breast cancer.

Purpose: The recent advent of a molecular MR (mMR) machine presents a unique opportunity to fuse PET data with the high soft-tissue contrast of MRI without the ionizing radiation of CT. Accurate measurement of FDG activity in PET requires attenuation correction (AC). CTAC is based on tissue density information provided by CT. MR signal is not dependent on tissue density, and thus mMR necessitates a method for MRAC. Current techniques for MRAC include the Atlas-based method and the Segmentation method. Validation of MRAC is required before comparisons can be made between SUVs derived from PET/CT using CTAC and those derived from PET/MRI using MRAC. We analyzed the relationship of SUV_{max} measured on PET/CT and PET/MRI using the Segmentation method with regards to 1) normal structures, 2) organ-specific breast cancer metastases, and 3) the ratio of SUV_{max} of organ-specific metastases to SUV_{max} of normal tissue. We also compared washout characteristics of normal structures and metastases.

Methods: For this HIPAA compliant, IRB approved prospective study, 30 women (age 37-75, mean 57) with n=1 newly diagnosed T2 and n=29 history of metastatic breast cancer underwent whole body (WB) 18-FDG PET/MR imaging on a commercially available 3T PET/MRI scanner (Siemens Biograph mMR) following routine clinical PET/CT. After WB gradient echo scout, a WB exam was conducted including 6-7 stations from thighs to vertex, with the following protocols per station: 1) 3D coronal VIBE Dixon for MRAC, 2) prototype T1 weighted radial 3D gradient echo (radial VIBE), and 3) 2D double-refocused echo-planar, diffusion weighted imaging [TR/TE=6000/65ms, FOV 450 mm, 2.3 x 2.3 x 6.0 mm voxel, SPAIR fat-suppression, three diffusion directions (3-scan trace), and b-values 0, 350, and 700 s/mm^2]. MR images were acquired prone with a set of flexible body matrix coils after rapid bolus injection of 0.1 mmol/L gadopentetate dimeglumine (Magnevist, Bayer)/kg body weight at 2.0 mL/sec IV prior to the first station. PET events were simultaneously accumulated for 6 minutes per station and images were reconstructed on the vendor platform incorporating u-maps from the AC scan. SUV_{max} was measured in 12 normal structures and in breast cancer metastases on PET/CT and PET/MRI from Mirada-64 (Mirada) by 2 readers using a 1mm^3 region of interest (ROI), with the exception of a 3mm^3 ROI for normal liver. Spearman rank correlation coefficients were calculated to look for systematic tendencies of CTAC and MRAC SUV_{max} to increase or decrease together. Two-tailed paired t tests were performed to look for potential differences between CTAC and MRAC SUV_{max}. A p-value < 0.05 was considered statistically significant.

Results: The mean uptake time following FDG injection was 62+15 minutes for PET/CT and 168+37 minutes for PET/MRI. For normal structures measured by reader 1, significant positive correlations were observed between CTAC and MRAC SUV_{max} in axillary nodes, bone, breast, renal cortex, inguinal nodes, and psoas muscle. For reader 2, significant positive correlations were seen in bone, breast, subcutaneous fat, psoas muscle, and spleen. For reader 1, MRAC SUV_{max} was significantly lower than CTAC SUV_{max} in 10 of 12 normal structures (adrenal gland, axillary nodes, breast, inguinal nodes, liver, lung, pancreas, renal cortex, spleen, and subcutaneous fat); no difference was observed in bone and psoas muscle. Results from reader 2 were identical with the exception of a trend towards statistical significance for axillary nodes (p=0.059). Regarding metastases, SUV_{max} was measured in a total of 30 lesions in 6 organs (only one metastasis per patient organ was measured). Bone (n=13), liver (n=6), and non-axillary lymph node (n=6) metastases were frequent enough for statistical analysis. Both readers observed a significant positive correlation between CTAC and MRAC SUV_{max} in bone lesions; a trend towards significance was seen in liver lesions (p=0.072 for both readers). MRAC SUV_{max} and CTAC SUV_{max} for metastatic lesions were not significantly different for either reader. The ratios of SUV_{max} of metastases to SUV_{max} of normal tissue were statistically similar between MRAC and CTAC for all organ-specific metastases. In the interval between PET/CT and PET/MRI, washout of radiotracer appeared accelerated in bone lesions compared to normal bone and delayed in non-axillary lymph node metastases compared to non-pathologic nodes, though statistical significance was not observed. Washout was significantly delayed in liver lesions compared to normal liver for reader 2 and trended towards significance for reader 1, as shown in Figure 1.

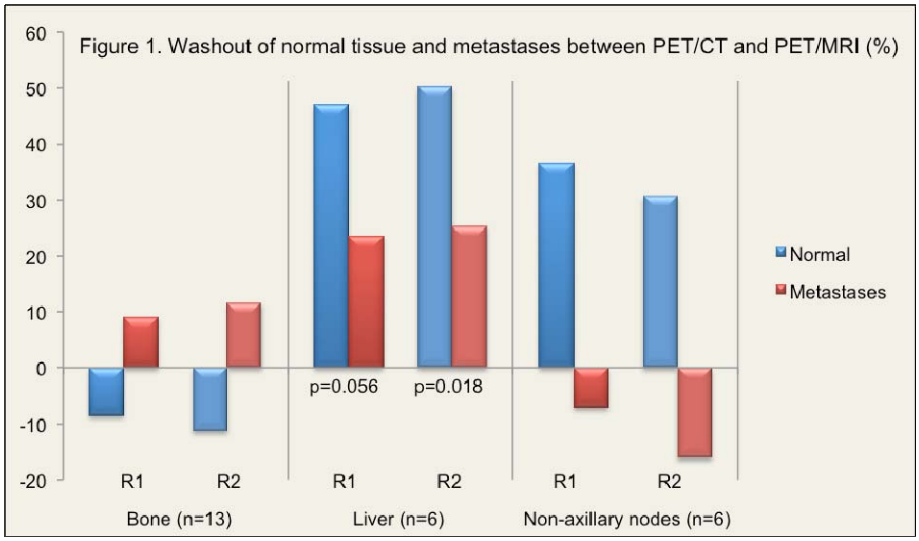

Discussion: SUV_{max} derived from MRAC correlates well with SUV_{max} derived from PET/CT for normal structures and breast cancer metastases, and the increase in SUV_{max} in metastases relative to normal tissue is similar using MRAC and CTAC. SUV_{max} derived from MRAC can thus be used for quantitative evaluation of FDG activity. In addition, breast cancer metastases demonstrate differential metabolic activity depending on the site of spread. Further studies are necessary to assess the role of SUV measurements in tailoring imaging to the metabolic activity of organ-specific metastases arising from various primary cancers.

Conclusion: SUV_{max} derived from MRAC can be used for quantitative evaluation of FDG activity.